Tropical Natural History 15(1): 41-54, April 2015


# Variations of Mammalian Cochlear Shape in Relation to Hearing Frequency and Skull Size

THANAKUL WANNAPRASERT[1] AND NATHAN JEFFERY[2]*

[1] *Department of Biology, Faculty of Science, Chulalongkorn University, Bangkok 10330, THAILAND*
[2] *Department of Musculoskeletal Biology, Institute of Ageing & Chronic Disease, University of Liverpool, Liverpool L69 3GA, UK*
* Corresponding authors. E-mail: njeffery@liverpool.ac.uk
Received: 24 September 2014; Accepted: 3 March 2015

**ABSTRACT.– The cochlea is the receptive organ of mammalian hearing and variations of its gross morphology have been linked to differences of hearing ability but as yet there has been little quantitative assessment of the proposed link, partly due to the difficulties of defining the complex geometry of the cochlea. The present study aims to quantitatively define the geometry and then determine whether adaptations of cochlear form are linked to the spatial limitations of the skull and hearing among a range of extant mammals. Advanced techniques in micro-CT imaging, 3D image visualization, geometric morphometrics and statistical methods were used to study the bony cochlea across 36 adult eutherian species. Data on hearing frequency were taken from the literature. Results showed that there was a considerable range of variation in form of the mammalian bony cochlea. The cochlear shape was correlated with the number of spiral turns. The low-frequency limit of hearing was negatively correlated with the cochlear length and volume. Also, the ratio of the intermeatal distance to cochlear length showed a correlation with the number of whorls and cochlear shape. It is concluded that the number of spiral turns is a key determinant of the eutherian cochlear shape. An increase in cochlear length and volume is likely to enhance low-frequency sound perception, whilst the cochlear spirals may not be related to hearing frequency. Results suggest that cochlear shape may be linked, at least in part, to the size of the skull either in terms of the wavelengths that can be used for localistion in smaller headed species and/or the demands of maintaining the physiological function of the cochlea in a smaller space.**

**KEY WORDS: cochlear shape; intermeatal distance; hearing frequency; spiral turns; morphology**

## INTRODUCTION

The coiled cochlea is a characteristic unique to therian mammals (marsupials and placentals). It was established after diverging from the monotremes during the Early Cretaceous period (Meng and Fox, 1995; Manley, 2000). The significance of the spiral form is not entirely clear. Morphologically, it is often thought to enable packing of a longer cochlea into the confines of the petrous bone. It is also suggested that coiling may allow acoustic nerve fibers to innervate different positions along the basilar membrane with the minimum of, and roughly equivalent, wiring lengths (West, 1985; Meng and Fox, 1995).

Coiling of the cochlea evolved together with an increase in the basilar membrane length. Functional implications of the elongated basilar membrane may be an overall extension of the frequency range (Meng and Fox, 1995; Luo et al., 2011; Manley, 2012), or an expansion of biologically significant frequency bands (acoustic foveae) as seen in, for example, some bats (West, 1985; Bruns et al., 1989). Hearing range in mammals expands towards both higher and lower frequencies compared to birds and reptiles (Popper and Ketten, 2007). West (1985) found a strong correla-

tion of low-frequency hearing with the product of basilar membrane length and the number of spiral turns. Meanwhile, Manoussaki et al. (2006, 2008) modeled the effects of spiral shape and proposed that cochlear curvature improves low-frequency sensitivity by focusing sound energy at the outer cochlear wall as waves propagate toward the apex. A recent study also suggested that the cochlear spiral geometry is related primarily to low-frequency energy focusing (Gavara et al., 2011). As yet however, these and other studies have relied on relatively simplistic representations of the cochlea geometry. This is partly due to the difficulties of capturing and then analysing its complex 3D form. Advances in computed tomography (CT), in particular micro-CT, coupled with readily available 3D rendering packages now allow for the capturing and recreation of the cochlea geometry in silico. Here we take the next step and outline a measurement and analytical strategy for investigating the geometry among eutherian mammals. Our specific hypotheses are that interspecific variations of cochlea form are linked to the spatial limitations of the skull and to hearing.

## MATERIALS AND METHODS

### Samples

The cochleae representing 36 extant eutherian mammals (one specimen per species) were included in the study (Table 1). The hearing data of the species studied were obtained from many different sources (Table 1). The data on the low frequency limit of hearing and best hearing frequency were available for 25 and 24 of the species studied, respectively. Thirty-two images of the whole skulls from Takahashi (2005) were downloaded and used for calculating the intermeatal distance (distance between the left and right external auditory meatuses) with ImageJ software (v. 1.42q; Rasband, 2012). The intermeatal distance was used as a proxy for the size of the skull.

### Micro-CT image processing and 3D image reconstruction

The inner ear of each specimen was non-invasively imaged with micro-CT. Isometric voxel resolutions ranged from 0.017 to 0.277 mm. Image data were then post-processed with ImageJ. Contiguous series of slice images were stacked to produce the entire volume of a 3D CT image. The grey-scale of the stack was inverted to make it easier to identify the void, representing the cochlear duct, rather than the surrounding bone. Image contrast was enhanced to accentuate the walls of the duct.

The processed image stacks were opened in Amira (v. 5.2.2; Visage Imaging, Germany). As the orientation of the petrous bone within the micro-CT machine can vary, the orientation of the slice planes was standardized by resampling the isometric image data in a plane parallel to the lateral semicircular canal (reference plane). The process of reconstructing 3D images was then performed; there are two operations—image segmentation and surface reconstruction. Image segmentation is the procedure of selecting voxels and then assigning these voxels to the inner ear. All segmentation was accomplished with a manual threshold value to define the bony outline of the cochlea canals and duct. Indistinct and/or complex boundaries (e.g., foramina) were determined by eye. For instance, the cochlea was separated from the tympanic cavity by linear boundaries created between two edges of the round window, and spanning the two edges of the oval window. Boundaries were

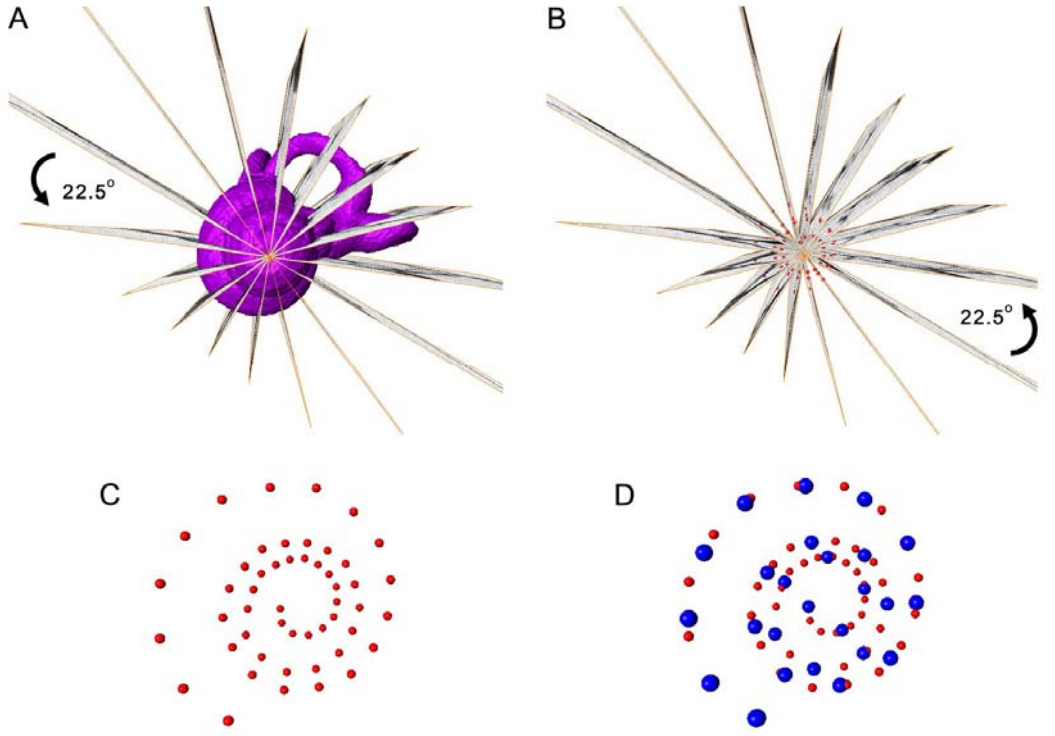


**FIGURE 1.** Landmark methods. **A** and **B**, the plane was rotated 22.5 degrees each to put landmarks around the mid-modiolar axis. Original landmarks (red) and 25 equidistant semi-landmarks (blue) were shown in **C** and **D**.

also created along the surfaces of the internal acoustic meatus and the modiolus to close off the numerous nerve foramina and to separate them from the cochlea. Next, polygonal surfaces of the inner ear were reconstructed and smoothed to generate 3D shells representing the cochlea.

## Measurement protocol

*Landmark methods*

A problem with landmarking the cochlea is its complex geometry. Any standard orthogonal plane will show only an oblique view of the duct's true cross section, thereby underestimating or overestimating its centre. To address this problem the cochlea data were resliced around a central axis, creating a series of images (like the spokes of a wheel) that remain perpendicular to the axis of the duct as its spirals. The central axis was set using a bespoke Amira module, and passed through the approximate mid-modiolar plane. It was decided that resliced planes every 22.5 degrees (16 per 360 degrees) would be sufficient for sampling the cochlea. Once each plane was rotated 22.5 degrees, landmarks were placed at the centre of the cochlear cavity (Fig. 1A, B). The start and end landmarks were standardized; the first landmark placed at the centre of the cavity in the plane showing the initial appearance of the inner osseous spiral lamina, and the end landmark was placed at the helicotrema (apex). This method captured the complex geometry of the cochlea

**TABLE 1.** Frequency and morphometric data in 36 eutherians studied.

| Species and abbreviation | Low-frequency limit (Hz)[a] | Best hearing frequency (kHz)[b] | Intermeatal distance (mm) |
|---|---|---|---|
| *Ailurus fulgens* (Af) | | | 56.92 |
| *Aotus trivirgatus* (At) | 125 | 10 | 24.97 |
| *Bos primigenius* (Bp) | 17 | 8 | 230.06 |
| *Camelus dromedaries* (Ca) | | | 133.16 |
| *Cannomys badius* (Cb) | | | 23.54 |
| *Castor canadensis* (Cc) | | | 73.69 |
| *Cavia porcellus* (Cp) | 47 | 8 | 20.02 |
| *Cebus apella* (Ca) | | | 42.41 |
| *Cryptomys hottentotus* (Ch) | 225 | 0.8 | 16.00 |
| *Cynomys ludovicianus* (Cl) | 13 | 4 | 27.03 |
| *Delphinapterus leucas* (Dl) | 40 | 70 | |
| *Eptesicus fuscus* (Ef) | 2600 | 20 | 7.73 |
| *Equus caballus* (Ec) | 42 | 2 | 82.42 |
| *Felis catus* (Fc) | 48 | 8 | 31.64 |
| *Galago senegalensis* (Gs) | 92 | 8 | 18.67 |
| *Hippopotamus amphibious* (Ha) | | | 177.86 |
| *Homo sapiens* (Hs) | 23 | 4 | 91.87 |
| *Lagostomus maximus* (Lm) | | | 53.57 |
| *Loxodonta africana* (La) | 17 | 1 | |
| *Lutra lutra* (Ll) | 450 | | 61.67 |
| *Marmota monax* (Ma) | 21 | 4 | 39.67 |
| *Mephitis* sp. (Me) | | | 33.06 |
| *Microtus pennsylvanicus* (Mp) | 1900 | 8 | |
| *Mirounga angustirostris* (Mi) | 75 | 6.4 | 156.00 |
| *Mus musculus* (Mm) | 2000 | 16 | 7.90 |
| *Myocastor coypus* (Mc) | | | 51.19 |
| *Odobenus rosmarus divergens* (Or) | 125 | 12 | |
| *Pedetes capensis* (Pe) | | | 30.60 |
| *Procyon lotor* (Pl) | 134 | 1 | 43.63 |
| *Rattus norvegicus* (Rn) | 290 | 32 | 16.94 |
| *Saimiri sciureus* (Ss) | 170 | 10 | 28.75 |
| *Talpa europaea* (Te) | 100 | 0.5 | 12.00 |
| *Tarsius bancanus* (Tb) | 1000 | 16 | 18.79 |
| *Trichechus senegalensis* (Ts) | 15 | 18 | 278.00 |
| *Tursiops truncatus* (Tu) | 200 | 65 | 173.66 |
| *Vulpes vulp*es (Vv) | | | 38.81 |

[a] The lowest frequency at which a mammal can detect. [b] The frequency with the lowest detection threshold.
[f] The audiogram of *Microtus arvalis*. [g] The audiogram measured in water.

but the number of landmarks varied among specimens according to the number of spirals and there was a spatial bias in the landmark density (i.e., morphologies closest to the rotational axis were represented by more landmarks than those further away from the axis). To offset bias, the original landmarks were used to create a set of 25 semi-landmarks at equidistant points from the start to end landmarks (Fig. 1C, D). These equidistant landmarks were then used in subsequent calculations and the geometric morphometric analyses.

*Measurement of the cochlear variables*

The cochlear variables measured included the number of cochlear turns, cochlear length and cochlear volume. The procedures

**TABLE 1.** continued.

| Cochlear variables | | | Audiogram source |
|---|---|---|---|
| **Spiral turns** | **Length (mm)** | **Volume ($mm^3$)** | |
| 2.125 | 15.115 | 24.416 | |
| 3.063 | 18.739 | 16.436 | Beecher, 1974b |
| 2.188 | 25.701 | 122.624 | Heffner and Heffner, 1983[c] |
| 2.313 | 28.918 | 121.886 | |
| 3.063 | 13.227 | 9.267 | |
| 2.750 | 17.942 | 41.138 | |
| 4.188 | 19.476 | 16.551 | Heffner et al., 1971 |
| 3.125 | 24.948 | 36.607 | |
| 3.375 | 10.346 | 2.854 | Bruckmann and Burda, 1997 |
| 3.563 | 13.291 | 7.914 | Heffner et al., 1994 |
| 2.000 | 35.403 | 157.902 | Nedwell et al., 2004 |
| 2.125 | 8.010 | 2.857 | Koay et al., 1997 |
| 2.438 | 31.346 | 114.865 | Heffner and Heffner, 1983 |
| 3.000 | 20.551 | 37.935 | Heffner and Heffner, 1985 |
| 2.750 | 13.517 | 12.630 | Heffner et al., 1969 |
| 3.125 | 44.503 | 317.127 | |
| 2.638 | 30.987 | 100.764 | Jackson et al., 1999 |
| 3.500 | 17.874 | 24.759 | |
| 2.250 | 35.796 | 322.715 | Heffner and Heffner, 1980[d] |
| 2.813 | 17.699 | 30.958 | Finneran and Jenkins, 2012[e] |
| 3.000 | 14.483 | 11.547 | Heffner et al., 2001 |
| 2.750 | 16.205 | 19.283 | |
| 2.500 | 7.042 | 2.268 | Lange et al., 2004[f] |
| 1.813 | 33.486 | 266.583 | Nedwell et al., 2004[g] |
| 1.875 | 5.213 | 1.420 | Koay et al., 2002 |
| 4.188 | 23.966 | 27.349 | |
| 2.500 | 32.369 | 352.861 | Nedwell et al., 2004[g] |
| 2.688 | 16.087 | 20.881 | |
| 2.500 | 18.355 | 41.980 | Wollack, 1965 |
| 2.438 | 8.207 | 4.183 | Heffner et al., 1994 |
| 2.938 | 19.708 | 20.319 | Beecher, 1974a |
| 2.000 | 5.439 | 1.655 | Aitkin et al., 1982 |
| 3.750 | 16.643 | 13.529 | Ramsier et al., 2012 |
| 1.750 | 30.713 | 342.215 | Nedwell et al., 2004 |
| 1.750 | 31.876 | 142.067 | Ketten, 1994 |
| 3.000 | 19.766 | 45.379 | |

[c] The audiogram of *Bos taurus*. [d] The audiogram of *Elephas maximus*. [e] The audiogram measured in air.

for measuring these variables were described as follows.

*Number of the cochlear turns*—the total number of original landmarks (not the equidistant set) from the first appearance of the inner bony lamina to the apex was used to calculate the number of the cochlear turns. Given $n$ total landmarks, the number of intervals between adjacent landmarks was $n$-1. As the former landmark was 22.5 degrees distant from the next, the total degree of the cochlear spiral was ($n$-1) × 22.5. To obtain the number of the cochlear turns, this total degree was divided by 360.

*Cochlear length*—the 3D length was computed as the sum of distances between

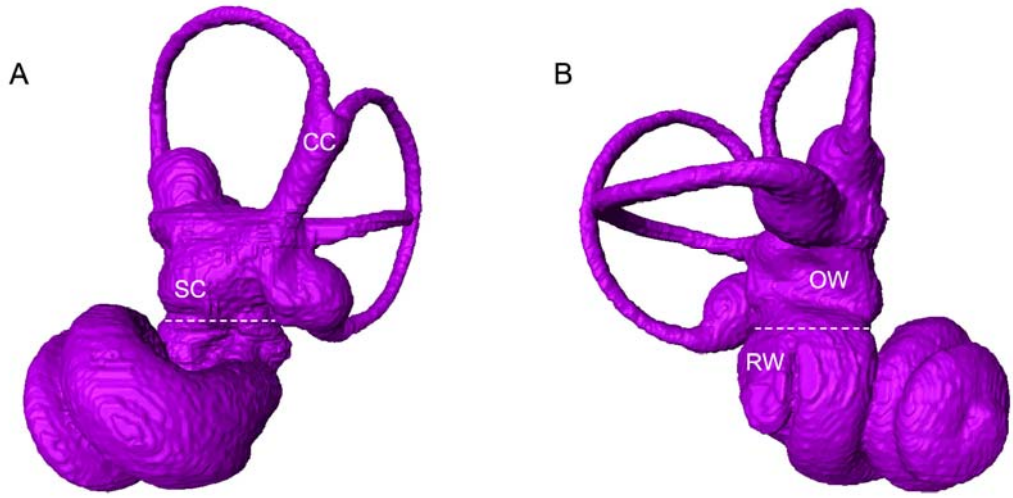


**FIGURE 2.** Measurement of the cochlear volume. The vestibular apparatus was removed from the cochlea. The boundary between them passed parallel to the groove under the saccular protrusion (**A**), and passed the first clear point of the inner osseous lamina, which was typically located between the oval and round windows (**B**). SC, saccule; OW, oval window; RW, round window; CC, common crus.

adjacent original landmark co-ordinates $[((x_2-x_1)^2 + (y_2-y_1)^2 + (z_2-z_1)^2)^{1/2}]$ (the 3D Pythagorean theorem) multiplied by voxel resolution.

*Cochlear volume*—all voxels of the inner-ear structures were loaded into Amira. The boundary between the cochlea and the vestibular apparatus was identified. The boundary passed parallel to the groove under the saccular protrusion, and passed the first clear point of the inner osseous lamina (Fig. 2). Voxels of the vestibular apparatus were then removed so that only voxels of the cochlea remained. The volume value was calculated as numbers of voxels multiplied by the volume ($mm^3$) of a single voxel.

*Shape analysis with geometric morphometrics*

The 3D coordinate data of the 25 semi-landmarks of all species were transposed into the Morphologika file format and imported into MorphoJ (v. 2.0) (Klingenberg, 2011). Data were subjected to a full Procrustes fit to minimise the effects of location, scale and rotation, leading to shape variables. The resulting hyper-dimensional covariance matrix representing differences among landmark configurations remaining after Procrustes superimposition was analyzed using Principal Component Analysis (PCA) to explore the general patterns of shape variation. A generally accepted cut-off criterion for examining PCs is 5% of the total variance (Zelditch et al., 2004). As the samples for the low-frequency limit, best hearing frequency and the intermeatal distance data differed, shape analysis was performed separately for comparison against each variable.

*Statistical analyses*

Data were examined using Spearman's rank correlation and reduced major axis (RMA) regression with PAST (v. 2.17b) (Hammer et al. 2001). Statistical signifi-

cance was accepted if the *P* value was less than 0.05. All variables except PC scores were log10-transformed prior to analysis. Comparisons made were as follows: the strength of the relationship between the cochlear shape (represented as PC scores) and the number of spiral turns was examined. The PC scores were obtained based on the data set of the low-frequency limit. Next, hearing parameters in relation to cochlear morphologies were investigated. The parameters used in the present study were the low-frequency limit of hearing and the best hearing frequency. The correlation and regression of the hearing parameters against the number of turns, the cochlear length and the volume, and the cochlear shape were performed. Also, a combination of the length and the number of spiral turns (length multiplied by the number of turns) was correlated against the low-frequency limit and compared with West's (1985) data. With regard to the role of the skull size in cochlear morphologies, the ratios of the intermeatal distance to the cochlear length (IMD/L) and the cochlear volume (IMD/V) were used to examine their relationships with the number of spiral turns and the cochlear shape. The cube root of the volume was used in the analyses to have the same scaling as the intermeatal distance.

## RESULTS

The mean number of the cochlear turns in 36 mammalian species studied was 2.72 ± 0.64 turns. The bottlenose dolphin (*Tursiops truncatus*) and the African manatee (*Trichechus senegalensis*) had the least number of cochlear turns (1.75 turns), whereas the most number of cochlear whorls was found in the coypu (*Myocastor coypus*) and the guinea pig (*Cavia porcellus*) at 4.2 turns.

**TABLE 2.** The percentage of the variance on each PC for each data set

| PC axis | Data set | | |
|---|---|---|---|
| | Low-frequency limit | Best hearing frequency | Intermeatal distance |
| PC1 | 44.7% | 44.4% | 41.2% |
| PC2 | 23.4% | 23.7% | 25.2% |
| PC3 | 12.1% | 11.8% | 11.5% |
| PC4 | 7.2% | 7.4% | 8.1% |

The general appearance of the cochlea among mammals was varied. Its overall shape ranged from the wide-based cochlea with a rounded apex in the toothed whales to the sharp-pointed, cone-shaped cochlea in the coypu and the guinea pig. In all the form analyses, PC1 through PC4 met the criterion that each one described 5% or more of the variance (Table 2). Total variance across all four components was 87.4% for the low-frequency sample, 87.3% for the best hearing frequency sample and 86% for the intermeatal distance sample.

For the relationship between the cochlear shape and the number of cochlear whorls, the results showed that only scores on PC1 were significantly correlated with the number of whorls ($r = -0.805$; $P < 0.001$). In other words, the number of turns was associated with 44.7% of the cochlear shape variation (Fig. 3A; Table 3).

Concerning the relationship between hearing ability and cochlear dimensions, the low-frequency limit of hearing was significantly negatively correlated with the cochlear length ($r = -0.536$; $P < 0.01$; Fig. 3B; Table 3) and volume ($r = -0.515$; $P < 0.01$; Fig. 3C; Table 3). The low-frequency limit also showed a significantly negative correlation with the combination of the length and the number of turns but the strength of the relationship was weaker (r =

**TABLE 3.** Significant Spearman's rank correlation and RMA regression found in the present study.

| Variables | n | r | Sig. | RMA regression | | |
|---|---|---|---|---|---|---|
| | | | | Slope | 95% CI | Intercept |
| log Number of Turns—PC1 scores | 25 | -0.805 | *** | -2.50 | (-3.05)-(-1.70) | 1.01 |
| PC4 scores—log Low-Frequency Limit | 25 | 0.476 | * | 6.49 | 3.72-8.41 | 2.05 |
| log Cochlear Length—log Low-Frequency Limit | 25 | -0.536 | ** | -2.63 | (-3.32)-(-1.82) | 5.30 |
| log Length x Spiral Turns—log Low-Frequency Limit | 25 | -0.476 | * | -2.53 | (-3.19)-(-1.40) | 6.20 |
| log Cochlear Volume—log Low-Frequency Limit | 25 | -0.515 | ** | -0.88 | (-1.10)-(-0.65) | 3.30 |
| log IMD/L—log Number of Turns | 32 | -0.46 | ** | -0.42 | (-0.51)-(-0.30) | 0.59 |
| log IMD/L—PC1 scores | 32 | 0.405 | * | 1.00 | 0.71-1.21 | -0.38 |
| log IMD/V—PC4 scores | 32 | -0.392 | * | -0.49 | (-0.64)-(-0.28) | 0.57 |

***P < 0.001; **P < 0.01; *P < 0.05

-0.476; $P < 0.05$; Fig. 3D; Table 3). By contrast, no significant correlation was found between the low-frequency limit and the number of turns. In relation to the cochlear shape, the low-frequency limit was significantly correlated with only PC4 scores that explained 7.2% of the total variance (r = 0.476; $P < 0.05$; Fig. 3E; Table 3). There is no significant correlation of the best hearing frequency with any of the cochlear variables.

The IMD/L ratio showed significant correlations with both the number of spiral turns (r = -0.460; $P < 0.01$; Fig. 3F; Table 3) and the shape variables on PC1 that explained 41.2% of the variance (r = 0.405; P < 0.05; Fig. 3G; Table 3). In contrast, the IMD/V had no significant correlation with the number of turns but showed a slightly weak relationship with PC4 scores accounting for 8.1% of the variance (r = -0.392; $P < 0.05$; Fig. 3H; Table 3).

## DISCUSSION

The number of cochlear turns varies considerably across eutherian species, ranging from 4.2 to 1.75 turns in the present study. The number of turns measured is similar to those documented previously (Watt, 1917; West, 1985; Solntseva, 2010; Ekdale, 2013). One exception is the guinea pig. Its cochlea had more turns than that the 3.5-3.75 turns reported by Wysocki's (2005) study. The 4.2 turns reported here, however, is consistent with other studies (e.g., West, 1985; Solntseva, 2010; Ekdale, 2013). The average number of spiral turns across all 36 species studied was 2.72 turns, which is similar to the study of Watt (1917), who reported an average of 2.6 whorls across 52 species. Interestingly, fully aquatic mammals studied so far tend to have the fewest whorls. Fewer spiral turns may be a key characteristic of species occupying a marine habitat. In addition, rodents show a great variation in the number of whorls, ranging from fewer than 2 turns of the mouse to more than 4 turns of the guinea pig and the coypu. Rodents exhibit a broad range of ecological niches and diverse behaviours. This variation may reflect the adaptation of the bony cochlea to hearing abilities in different environments and social structures.

In the present study, the cochlear length was measured and its values were relatively smaller than the basilar membrane length

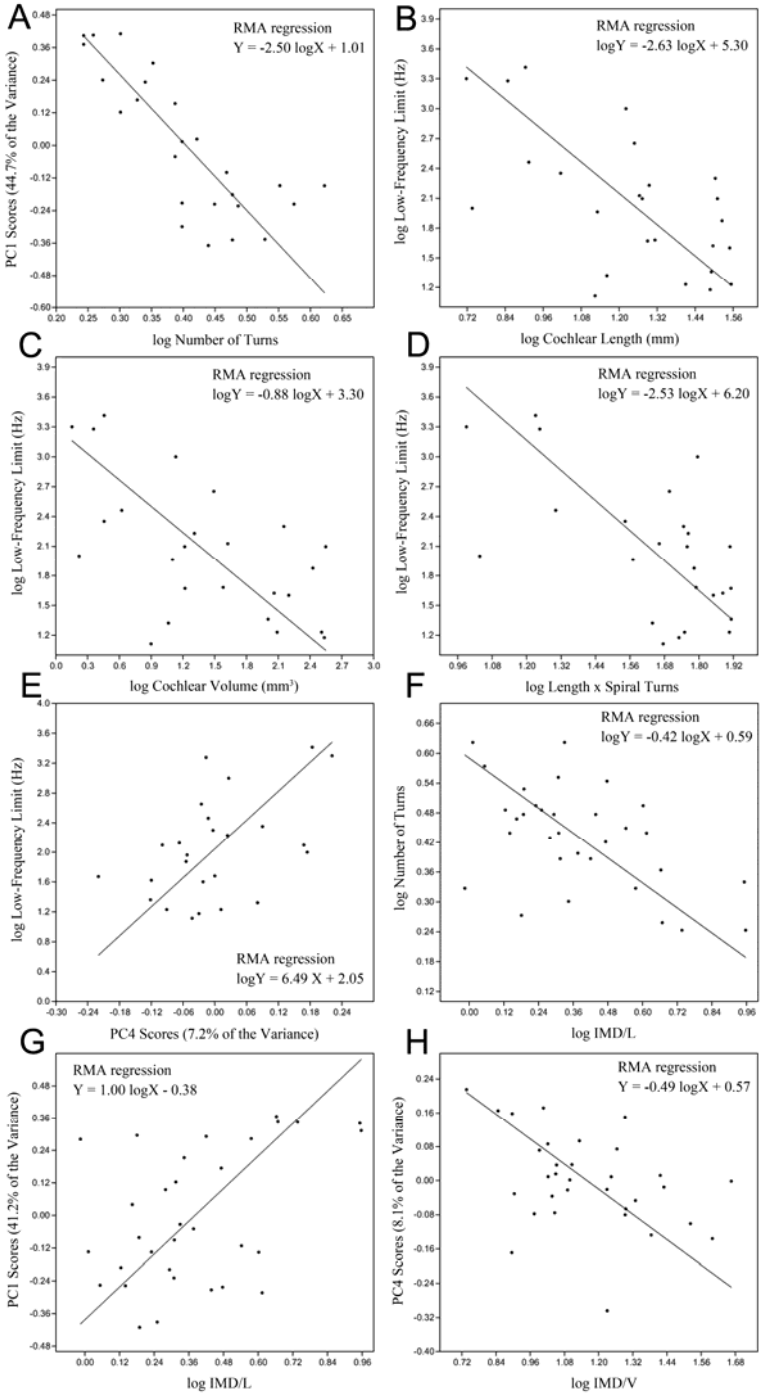


**FIGURE 3.** Scatter plots (**A** to **H**) of all significant correlations that were found in the present study.

reported in previous studies (West, 1985; Manoussaki et al., 2008). These different results are probably due to the fact that the basilar membrane is located near the outer edge of the cochlear cavity, compared with the measurement point of the cochlear length at the centre of the cavity. This also explains why the values in the present study were relatively shorter when compared with the cochlear length data of Coleman and Colbert (2010), which were measured along the outer circumference of the cochlea. Concerning the cochlear volume, previously published data is scarce and mostly available for primates. The volumes in primate samples measured in the present study were different from those for five species reported in Kirk and Gosselin-Ildari (2009). This discrepancy is perhaps due to different procedures and criteria in determining the cochlear border from unwanted surrounding structures.

The finding that the number of spiral turns was strongly correlated with PC1 scores corresponds with the pattern of shape variation described by PC1. The PC1 axis accounted for almost half a total variance and primarily represented changes in the number of cochlear whorls and also the radius of curvature at the basal cochlear part (Fig. 4). Therefore, the present study suggests that the number of turns is one of the main factors associated with cochlear shape determination.

The spiral shape is often thought to facilitate packing a long cochlea into a limited space of the skull, and to increase the efficiency of neurovascular supply of an elongated receptor surface (Von Bekesy, 1960; Meng and Fox, 1995). Debate concerning the selective advantages of coiling on hearing among mammals persists. Some authors argued that the cochlear curvature appears to have very little effect on the hearing sensitivity (Von Bekesy, 1960; Loh, 1983), whilst others reported that the cochlear curvature may promote sensitivity to low-frequency sounds (Manoussaki et al., 2006, 2008; Gavara et al., 2011). Among echolocating species (toothed whales and bats), the number of coils does not support a link with the perceived frequency range (Fleischer, 1976; Solntseva, 2010). In the present study, the number of whorls did not show a significant correlation with either low-frequency limit or best hearing frequency. Moreover, only a slight correlation was detected between the low-frequency limit and scores on PC4, which did not principally describe shape variation related to changes in the number of spiral turns but the elongation of the cochlea. Based on these results, the present study does not support the hypothesis about the association between the cochlear spiral geometry and improved low-frequency audition.

The present study found a negative correlation between the cochlear length and the low-frequency limit. In other words, species with a longer cochlea favour the frequency range tuned towards lower frequencies. This finding agrees with the results from many researchers (West, 1985; Burda et al., 1989; Begall et al., 2007; Coleman and Colbert, 2010). An increase in cochlear length may accommodate more hair cells along its receptor surface. The increased number of hair cells is associated with either an extension of the frequency range or a greater frequency discrimination at a given relevant frequency band (Bruns et al., 1989; Coleman and Colbert, 2010). In addition, Watt (1917) supposed that the elongation from the typical length of the mammalian cochlea is mainly caused by an accretion at the apex, not the basal region. Therefore, the present study suggests that an

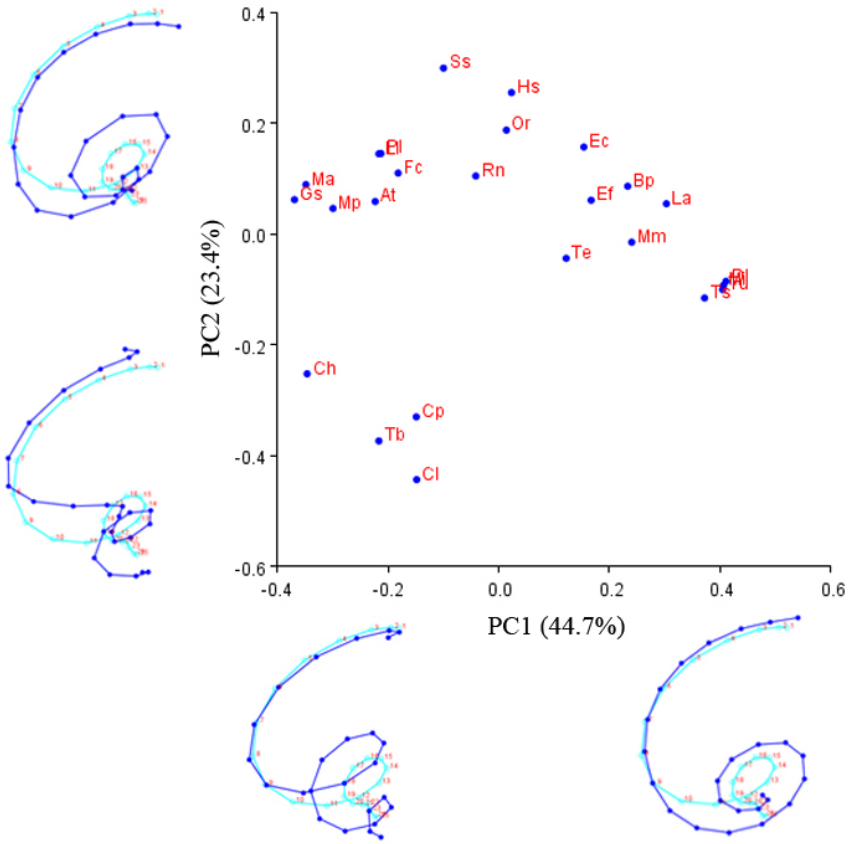


**FIGURE 4.** Shape variation of the mammalian cochleae described by the scatter plot of PC1 vs PC2. The pattern of shape variability represented by each PC was indicated by the constructed cochlear wireframes. The light blue lines indicated the mean shape (the coordinate (0.0, 0.0)) and the dark blue lines showed the shape at the extreme of each axis. The species abbreviations were shown in Table 1.

increased length may provide space for more hair cells in the apical region where low frequency sound is primarily perceived, hence enhanced low-frequency response.

A negative correlation was also noted between the cochlear volume and the low-frequency limit. This result agrees with previous studies in primates (Kirk and Gosselin-Ildari, 2009; Armstrong et al., 2011), and indicates that the low-frequency limit decreases with increasing cochlear size. Information about the mammalian cochlear volume, however, is scarce and its impact on hearing abilities is still questionable. One can speculate that the mass and pressure oscillation of cochlear fluids may have a resonant effect on frequency analysis along the cochlear duct. The exact mechanisms accounting for this relationship remain to be clarified.

That a mammal has a highly coiled cochlea or a flattened cochlea with few turns could be partly due to the spatial limitations of skull. If the area for expansion of the basal turn is limited, an elongation of the cochlea length can be accomplished by

increased spiralization (Bruns et al., 1989). The IMD/L reflects the size of the skull relative to the cochlear length; the lower the ratio, the more limited skull space for cochlear expansion is. The present study found that the IMD/L was negatively correlated with the number of spiral turns. In other words, the number of turns tends to decrease when the IMD/L ratio increases. Based on this result, the present study suggests that an adequate space within the skull (probably petrous bone size) may provide for the untwisting of the basal cochlear turn, leading to a decreased number of turns. The finding that the IMD/L was correlated with PC1 scores supports the notion that architectural constraints of the skull may affect spiraling, which in turn influences cochlear shape variation. The IMD/V was not correlated with the number of turns and showed only a slight correlation with PC4. Further work, incorporating petrous bone size into the analysis as well and focusing on smaller species, in which size limits are more pronounced, is needed to clarify the relationship between spatial constraints of the skull and the cochlear shape. It is worth noting that the cochlea in many species achieves adult size early on in development (Jeffery and Spoor, 2004; Solntseva, 2010). Thus, it might be that skull size reached once the cochlea reaches full size that dictates this spatial relationship not adult skull size—that is the cochlea may appear small relative to the adult skull but that does not exclude the notion that there was a pinch point earlier on in development when the skull was much smaller.

In summary, the number of spiral turns is a main determining factor of the bony cochlear shape in eutherians. The spiral form of the cochlea is not related to an extension of frequency range towards lower frequencies. By contrast, the cochlear volume and length are associated with improved low-frequency hearing. Physical properties of cochlear fluid are surmised to have an effect on cochlear tuning. An increase in cochlear length may occur at the apex, which accommodates more hair cells that respond best to low-frequency sounds. Finally, the skull size may impose a condition of the cochlear spirals and subsequently affect the cochlear shape.

## ACKNOWLEDGEMENTS

This project is supported and funded by Ministry of Science and Technology, Thailand. We would like to convey thanks to several museums for providing skull specimens and to The University of Manchester for micro-CT imaging. We also thank Dr. Philip Cox for advice on morphometric techniques and for micro-CT image files of rodent inner ears.

## LITERATURE CITED

Aitkin, L.M., Horseman, B.G. and Bush, B.M.H. 1982. Some aspects of the auditory pathway and audition in the European mole, *Talpa europaea*. Brain Behavior and Evolution. 21: 49-59.

Armstrong, S.D., Bloch, J.I., Houde, P. and Silcox, M.T. 2011. Cochlear labyrinth volume in Euarchontoglirans: implications for the evolution of hearing in primates. Anatomical Record. 294: 263-266.

Beecher, M.D. 1974a. Pure tone thresholds of the squirrel monkey (*Saimir sciureus*). Journal of the Acoustical Society of America. 55: 196-198.

Beecher, M.D. 1974b Hearing in the owl monkey (*Aotus trivirgatus*): I. auditory sensitivity. Journal of Comparative and Physiological Psychology. 86: 898-901.

Begall, S., Lange, S., Schleich, C.E. and Burda, H. 2007. Acoustics, audition and auditory system. In: Begall S, Burda H, Schleich CE (eds.) Subterranean rodents: news from underground. Springer-Verlag, Berlin, pp 97-111.

Bruckmann, G. and Burda, H. 1997. Hearing in blind subterranean Zambian mole-rats (*Cryptomys* sp.):

collective behavioural audiogram in a highly social rodent. Journal of Comparative Physiology A. 181: 83-88.

Bruns, V., Burda, H. and Ryan, M.J. 1989 Ear morphology of the frog-eating bat (*Trachops cirrhosus*, Family: Phyllostomidae): apparent specializations for low-frequency hearing. Journal of Morphology. 199: 103-118.

Burda, H., Bruns, V. and Nevo, E. 1989. Middle ear and cochlear receptors in the subterranean mole-rat, *Spalax ehrenbergi*. Hearing Research. 39: 225-230.

Coleman, M.N. and Colbert, M.W. 2010. Correlations between auditory structures and hearing sensitivity in non-human primates. Journal of Morphology. 271: 511-532.

Ekdale, E.G. 2013. Comparative anatomy of the bony labyrinth (inner ear) of placental mammals. PLoS ONE. doi:10.1371/journal.pone.0066624.

Finneran, J.J. and Jenkins, A.K. 2012. Criteria and thresholds for U.S. Navy acoustic and explosive effects analysis. SSC Pacific, USA.

Fleischer, G. 1976. Hearing in extinct cetaceans as determined by cochlear structure. Journal of Paleontology. 50: 133-152.

Gavara, N., Manoussaki, D. and Chadwick, R.S. 2011. Auditory mechanics of the tectorial membrane and the cochlear spiral. Current Opinion in Otolaryngology & Head and Neck Surgery. 19: 382-387.

Hammer, Ø., Harper, D.A.T. and Ryan, P.D. 2001. PAST: paleontological statistics software package for education and data analysis. Palaeontologia Electronica. 4: 1-9.

Heffner, H.E., Heffner, RS., Contos, C. and Ott, T. 1994. Audiogram of the hooded Norway rat. Hearing Research. 73: 244-248.

Heffner, H.E., Ravizza, R.J. and Masterton, B. 1969. Hearing in primitive mammals, IV: bushbaby. Journal of auditory research. 9:19-23.

Heffner, R. and Heffner, H. 1980. Hearing in the elephant (*Elephas maximus*). Science. 208: 518-520.

Heffner, R. and Heffner, H. 1983. Hearing in large mammals: the horse (*Equus caballus*) and cattle (*Bos taurus*). Behavioral Neuroscience. 97: 299-309.

Heffner, R. and Heffner, H. 1985. Hearing range of the domestic cat. Hearing Research. 19: 85-88.

Heffner, R., Heffner, H., Contos, C. and Kearns, D. 1994. Hearing in prairie dogs: transition between surface and subterranean rodents. Hearing Research. 73: 185-189.

Heffner, R., Heffner, H. and Masterton, R.B. 1971. Behavioral measurement of absolute and frequency-difference thresholds in guinea pig. Journal of the Acoustical Society of America. 49: 1888-1895.

Heffner, R., Koay, G. and Heffner, H. 2001. Audiograms of five species of rodents: implications for the evolution of hearing and the encoding of pitch. Hearing Research. 157: 138-152.

Jackson, .LL., Heffner, R.S. and Heffner, H.E. 1999. Free-field audiogram of the Japanese macaque (*Macaca fuscata*). Journal of the Acoustical Society of America. 106: 3017-3023.

Jeffery, N. and Spoor, F. 2004. Prenatal growth and development of the modern human labyrinth. Journal of Anatomy. 204: 71-92.

Ketten, D.R. 1994 Functional analyses of whale ears: adaptations for underwater hearing. IEEE Proceedings Underwater Acoustics. 1: 264-270.

Kirk, E.C., Gosselin-Ildari, A.D. 2009. Cochlear labyrinth volume and hearing abilities in primates. Anatomical Record. 292: 765-776.

Klingenberg, C.P. 2011. MorphoJ: an integrated software package for geometric morphometrics. Molecular Ecology Resources. 11: 353-357.

Koay, G., Harrington, I.A., Heffner, R.S. and Heffner, H.E. 2002. Audiograms of mice lacking Scn8a sodium channels and their heterozygous littermates. Hearing Research. 171: 111-118.

Koay, G., Heffner, H.E. and Heffner, R.S. 1997. Audiogram of the big brown bat (*Eptesicus fuscus*). Hearing Research. 105: 202-210.

Lange, S., Stalleicken, J. and Burda, H. 2004. Functional morphology of the ear in fossorial rodents, *Microtus arvalis* and *Arvicola terrestris*. Journal of Morphology. 262: 770-779.

Loh, C.H. 1983. Multiple scale analysis of the spirally coiled cochlea. Journal of the Acoustical Society of America. 74: 95-103.

Luo, Z.X., Ruf, I., Schultz, J.A. and Martin, T. 2011. Fossil evidence on evolution of inner ear cochlea in Jurassic mammals. Proceedings of the Royal Society, B. 278: 28-34.

Manley, G.A. 2000. Cochlear mechanisms from a phylogenetic viewpoint. Proceedings of the National Academy of Sciences of the USA. 97: 11736-11743.

Manley, G.A. 2012. Evolutionary paths to mammalian cochleae. Journal of the Association for Research in Otolaryngology. 13: 733-743.

Manoussaki, D., Chadwick, R.S., Ketten, D.R., Arruda, J., Dimitriadis, E.K. and O'Malley, J.T.

2008. The influence of cochlear shape on low-frequency hearing. Proceedings of the National Academy of Sciences of the USA. 105: 6162-6166.

Manoussaki, D., Dimitriadis, E.K. and Chadwick, R.S. 2006. Cochlea's graded curvature effect on low frequency waves. Physical Review Letters. 96: 088701.

Meng, J. and Fox, R.C. 1995. Osseous inner-ear structures and hearing in early marsupials and placentals. Zoological Journal of the Linnean Society. 115: 47-71.

Nedwell, J., Edwards, B., Turnpenny, A.W.H. and Gordon, J. 2004. Fish and marine mammal audiograms: a summary of available information. Subacoustech, Hampshire.

Popper, A.N. and Ketten, D.R. 2007. Handbook of the senses. Elsevier, Oxford.

Ramsier, M.A., Cunningham, A.J., Moritz, G.L., Finneran, J.J., Williams, C.V., Ong, P.S., Gursky-Doyen, S.L. and Dominy, N.J. 2012 Primate communication in the pure ultrasound. Biology Letter. 8: 508-511.

Rasband, W.S. 2012. ImageJ. http://imagej.nih.gov/ij/. Accessed 1 March 2014.

Solntseva, G.N. 2010. Morphology of the inner ear of mammals in ontogeny. Russian Journal of Developmental Biology. 41: 94-110.

Takahashi, H. 2005. Mammalian Crania Photographic Archive. http://1kai.dokkyomed.ac.jp/mammal/en/index_sci.html. Accessed 28 March 2014.

Von Bekesy, G. 1960 Experiments in hearing. McGraw Hill, New York.

Watt, H.J. 1917. The typical form of the cochlea and its variations. Proceeding of the Royal Society of London, B. 89: 410-421.

West, C.D. 1985. The relationship of the spiral turns of the cochlea and the length of the basilar membrane to the range of audible frequencies in ground dwelling mammals. Journal of the Acoustical Society of America. 77: 1091-1101.

Wollack, C.H. 1965. Auditory thresholds in the raccoon (*Procyon lotor*). Journal of auditory research. 5: 139-144.

Wysocki, J. 2005. Topographical anatomy of the guinea pig temporal bone. Hearing Research. 199: 103-110.

Zelditch, M.L., Swiderski, D.L., Sheets, H.D. and Fink W.L. 2004. Geometric morphometrics for biologists: a primer. Elsevier Academic Press, San Diego.